

Vascular texture modeling for image interpretation

MAREK KRĘTOWSKI^{1,2}, JOHANNE BÉZY-WENDLING²

¹Department of Computer Science, Technical University of Białystok, Białystok, Poland

²Laboratoire Traitement du Signal et de l'Image, INSERM, Université de Rennes 1, Rennes, France

In this paper, it is shown that pathological changes of vascular networks, inside an extensive organ, influence textures observed on medical images. A 3D, dynamic model of the organ and its vascular system was developed, and it enables to control the tissue perfusion. To render CT scan-like images, the acquisition process was also modeled. The proposed approach is applied to simulate the development of the hepatic vascular system and to induce hyper- and hypo-vascularized lesions inside the liver. The texture analysis of the obtained images is then performed. It shows that textural features can characterize regions changed by pathological processes as far as the acquisition conditions are precisely controlled.

Keywords: medical imaging, texture analysis, vascular modeling

Corresponding author:

Marek Krętowski
Department of Computer Science
Białystok Technical University
Wiejska 45A, 15-351 Białystok
fax: (085) 7-423-423
e-mail: mkret@ii.pb.bialystok.pl

1. Introduction

Rapid scientific and technological progress enables to obtain better, more detailed medical images with each forthcoming generation of the imaging equipment. New, faster and less invasive possibilities to explore. In many situations, nowadays it is difficult even to imagine a reliable diagnosis without the support of imaging information. Moreover, computer-supported methods for image analysis become increasingly powerful, and they become more and more frequently applied in clinical practice. Nevertheless, semi-automatic and objective tissue characterization still remains an open problem for many types of imaging modalities and organs.

The texture analysis is a useful tool in describing homogeneous areas of medical images. It consists in extracting a set of parameters, to characterize Regions Of Interest (ROI) defined in the concerned organs. These features are generally derived from simple (e.g. first-order and gradient-based statistics) or more sophisticated (for example, based on co-occurrence or run-length matrices) statistical properties of the image. Another possibility is model-based approaches (e.g. fractals and Markov fields), transform methods (e.g. based on Fourier, Gabor or wavelet transformations) and mathematical morphology operations.

Texture analysis is known to be a very sensitive method in discrimination of pathologies [1]. It was successfully applied in a broad range of imaging modalities and diagnostic problems such as dystrophy of the skeletal muscle (MRI) [2], breast nodules (ultrasound B-scan) [3], botulism on trabecular bone (X-ray radiograms) [4], solitary pulmonary nodules (CT) [5], coronary plaques (intravascular ultrasound) [6] (for an exhaustive literature review in medical applications, refer to [1]). Even if all these works lead to potentially interesting results, common difficulties raise. The number of potential textural features is high, and it is generally not easy to choose the most relevant ones given the organ, its pathology and the imaging modality, especially for doctors without a great experience in texture analysis. Straightforward mapping of the extracted parameters to image characteristics used by radiologists during their visual analysis are not always possible, and this may explain why these automatic methods are not extensively used in clinical routine. Another difficulty lies in the lack of standardization of methods used to acquire and analyze images, which makes difficult any reliable comparison of the results obtained in various centers. The need to define appropriate protocols is unquestionable, but achieving the consensus is very difficult, especially because it depends on the acquisition equipment. This situation emphasizes the difficulties to control and reduce the variability of the features as reported in the literature.

In order to face aforementioned problems and to better understand the relation between observed image data and underlying tissue properties computational modeling of the texture formation process is useful. In such approach, two coupled models have to be created: the model of the extensive organ concerned and the model of the chosen image modality. More specifically, models of the liver and the computer tomography (CT) scanner are combined. This way, it is possible to control the full process of the image formation (see the steps I and II in Figure 1). Even if modeling remains only an approximation of reality, it offers many advantages. First, it is possible to scan repeatedly the same organ by just changing the acquisition conditions, which is not feasible during the patient examination. Second, many pathological modifications can be studied only by changing the model parameters.

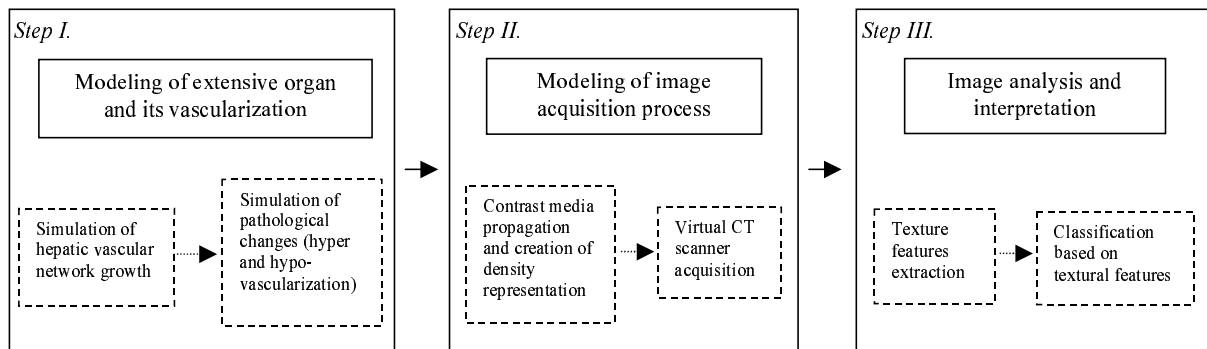


Figure 1. Scheme of the modeling-based approach for medical image analysis.

When considering the liver, important vascular modifications appear in a number of diseases, leading to generally visible patterns on CT scans, especially when structure enhancement techniques (like the contrast media injection) are applied. It is why the vascular system model is the most important component of our methodology.

Many experimental and theoretical contributions have been developed in order to understand the principles governing the vessels' development and to formalize this process (see e.g. work of Murray [8]). Recently, the idea of computer modeling of the vascular tree growth has become feasible due to significantly increased computational power. 2D simple models were developed (e.g. [8], [9], [10]) and replaced soon afterwards by much more realistic 3D simulations (e.g. [11]). The predecessor of the vascular model used in the present study was introduced in [12] and has evolved gradually since that time.

This study can be seen as a continuation of [14], where the ideas originally proposed in [13] were investigated. In comparison to the previous works, both involved models (i.e. organ and CT modality) have been significantly improved (single arterial tree have been replaced by the vascular network of three functionally connected trees, the contrast media enhancement has been modeled, the image resolution has been increased, ...).

The remaining sections of the paper is organized as follows. In the first part of the next section, the model of tissue and the vascular network that perfuses it is presented. In the second part, the model of CT scanner modality is described. In section 3, all experimental results are highlighted. The growth of the hepatic vascular system in the normal condition and the development of tumor-like lesions are illustrated. Then, the influence of the pathological processes on textures observed on the simulated CT scans is investigated. Short conclusions and future plans follow in the last section.

2. Presentation of the coupled models

The generic model of a given extensive organ (in which all cells are able to divide all along their life, allowing the organ to increase its size) has to be adapted to the specificity of the organ under consideration, the liver, especially in parts dealing with the blood supply. In addition, the model of the CT scan acquisition has to take into account some particularities of the contrast media propagation in liver in order to obtain more realistic images.

2.1. Model of liver

The model is designed to simulate the growth of the liver and certain pathological processes, which can take place inside the organ. Two phases can be distinguished: the “growth phase”, when the external shape expands gradually and the “adult phase”, when the size of the organ does not change. In the first phase a simulation is initiated with an organ, whose size is a small fraction of the one of an adult liver, and continues until it reaches the full size. The changes in the size and the structure of the organ operate at discrete time moments called (sub-) cycles. The modeled liver consists of two main components: the tissue (which corresponds to the parenchyma) and the vascular network that perfuses it. The tissue is represented by a set of macro-cells evenly (but in a random manner) distributed inside the external organ shape. Each macro-cell is a small, fixed size part of the tissue, and constitutes the functional unit of the model. It is characterized by a spatial, relative position inside the shape, and by its class, which determines most of functional/structural properties (e.g. probability of mitosis/necrosis: P_m/P_n) and physiological features (e.g. blood flow rate). Several classes of macro-cells can be defined to differentiate functional (or pathological) regions of tissue. Furthermore, the class of macro-cells can be changed during their lifetime, and this property offers a natural framework to simulate the evolution of a given disease (e.g. tumor). Certain parameters (like blood flow rate) associated with the macro-cell’s class are described by their distribution, and they are randomly chosen for each new macro-cell (e.g. this is the case for the terminal flow, whose natural variability is modeled in such a way).

During the “growth phase”, the external shape of the modeled organ expands periodically (at cycles). Because the relative position of macro-cells remains unchanged, it leads to the apparition of parts of the tissue which are not represented by any macro-cell. These spaces are filled by new macro-cells in consecutive sub-cycles which are repeated until the equilibrium is reached between the number of new macro-cells and the number of dying ones. In each sub-cycle, a macro-cell can divide (with a probability P_m) into two macro-cells of the same class. The new macro-cell’s position is chosen randomly in the neighborhood of the “mother” but created only if the local constraints of maximal density and minimal distance for all macro-cells are fulfilled. The macro-cell can also die at each sub-cycle according to a given probability (P_n).

The tissue is perfused by a vascular network, which is composed of three vascular trees with blood going from the arterial and portal trees to the venous one through macro-cells (Fig. 2). The macro-cells correspond to capillaries of real vascular system, and they play the main role in exchanges of oxygen, carbon dioxide and nutrients (this process is not modeled).

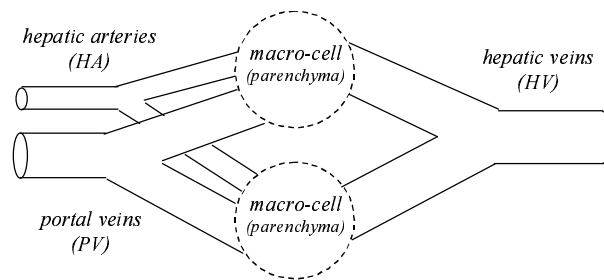


Figure 2. Specificity of the hepatic vascular system lies in the dual blood supply by hepatic artery and portal vein.

Any real vascular network is composed of vessels that divide (or merge) creating bifurcation. In the presented model, the vascular trees are binary ones (*anastomoses* are not taken into account) with nodes characterized by their spatial position and their blood flow rate and pressure. Each vessel segment is an ideal tube with the wall thickness depending on the vessel radius and function (artery or vein). Blood is regarded as a Newtonian fluid, with constant viscosity, whose flow is governed by *Poiseuille’s law* (which relates the pressure difference between two extremities of a vessel with the blood flow rate, length and radius of the vessel). At each bifurcation the *law of matter preservation* has also to be fulfilled (the quantity of blood, which enters a bifurcation, leaves it). Another constraint deals with the decreasing vessel radii in the vascular tree (the *bifurcation law*) giving the relationship between the radius of the mother vessel and radii of its two daughters.

Newly appeared macro-cells are *ischemic*, because they are not perfused by the existing vascular system, and they signalize this by secreting some *angiogenic factors* (AF). In

response to this chemical stimulus the closest vessels, situated in the neighborhood of a new macro-cell, sprout toward the macro-cell [15]. In fact, to perfuse the macro-cell each “candidate” vessel creates a new bifurcation, and then the branching position is searched. The optimality principle [16] is commonly accepted in vascular modeling and the minimal blood volume is applied to guide such a search in our model (arguments leading to the choice of the blood volume can be found in [17]). The method proposed in [18] was adapted to 3D situation, to find the geometry of the bifurcation (see [12] for details, in case of a single tree). The next step is devoted to a recalculation of vessel’s characteristics (i.e. blood flow, pressures and radii) in the whole tree to fulfill all constraints (i.e. physical and physiological laws). A method called “fast updating” was developed [19] in order to accelerate this time consuming operation.

The above process can be regarded as a kind of competition, because only one vessel in each tree will perfuse the macro-cell and the remaining vessels have to retract before disappearing. In each tree, the configuration leading to the lowest volume of the whole tree should be chosen, in order to be consistent with the optimality principle of minimal blood volume. Furthermore, the problem of avoiding possible collisions among vessels has also to be taken into account, especially in the case of crossing among arteries (arterioles) and veins (venules). These two constraints lead to a simple algorithm, in which the non-crossing combination of candidates from each tree with the lowest sum of blood volumes is chosen. However, more sophisticated procedures based on the conformation corrections (e.g. bypassing) in case of undesirable intersections can be developed.

As it has been already mentioned, the macro-cell can also die and then the situation is reversed: all vessels supplying the macro-cell retract and disappear. The corresponding bifurcations are reduced to single vessels or two segments connected in the former bifurcation points.

Usually (in normal condition, i.e. healthy tissue), the class of macro-cell remains unchanged during all the life of the macro-cell, but can be modified (e.g. to simulate the pathological process inside the organ). The model offers the possibility to define sequences of so called *conversions*. Each conversion represents the period when the current class of macro-cells inside the chosen region (e.g. sphere) can be changed (with the given probability) to another class. The sequence enables to model for instance various stages of pathology development, when macro-cells characteristics evolve gradually. Furthermore, conversions can operate in parallel way in different part of the tissue to simulate multiple lesions. After the initiation of the pathological region by using the conversion, the disease develops during

consecutive cycles leading to spatial/density changes in tissue and especially in its vascularization.

2.2. Modeling the CT scan acquisition

The second step of the methodology deals with the CT scan modality. Before the acquisition simulation, the 3D density representation of the scanned organ is created. In case of abdominal organs (like e.g. liver or kidney) the structure enhancement technique (i.e. contrast material injection), which is usually applied before imaging, has also to be modeled. In clinical practice, the contrast material is injected intravenously (e.g. into the *antecubital vein*), and after a bolus transfer time, it reaches the liver first through the hepatic artery and then, with a certain delay, through the portal vein. The curves corresponding to the propagation of the Contrast Material (CM) in HA and PV belong to the parameter set of the model. The CT scans are generated as time-stamped sequences, but each image is static. It means that instead of simulating the full propagation of CM, it is sufficient to compute the distribution of the concentration inside the organ at different acquisition instants. The time taken by the CM (ideally mixed with the blood) to go from the input of the tree to each vessel is known, using the physiological and geometrical characteristics of the vessels. For each vessel, the CM concentration can be calculated at a considered time, given the delay taken by the CM to arrive into the vessel, and the concentration curves at the input of the tree. The evolution of the CM concentration in the parenchyma is also computed, depending on the respective CM quantities in the arteriole and the portal venule, supplying the macro-cell. The density of parenchyma depends on the value associated with the class of the macro-cell and is increased by using the contrast media. Similarly, the density of the vessel is proportional to CM level in the blood. Moreover, when the vessel intersects the voxel the partial volume effect is taken into account. To render the spatial variation of parenchyma and the heterogeneity of CM, the obtained densities are modified by adding small fluctuations.

Based on the density representation, a standard CT scanner acquisition is simulated (i.e. parallel geometry). The most important parameters, which can be modified, include the scan position, slice thickness and image resolution. X-ray projections are computed (using the Radon transform) for all considered angles. Then, to reconstruct the image, a filtered back-projection algorithm ([20], [21]) is applied. In our implementation, the simple band-limited $|\omega|$ filter in Fourier domain is used.

3. Experimental results

Programs used in image modeling and texture analysis were implemented in C++ and all the simulations were performed on a PC (Pentium II 350MHz, 512MB RAM).

3.1. Growth of the hepatic vascular network

The growth of the hepatic vascular system is first simulated in normal conditions. The main parameters of the model are given in table 1 (average physiological values correspond to normal conditions). The external liver envelope was defined earlier from a set of 2D CT slices. The main branches (7 segments) of each tree are initialized according to standard positions (taken from an anatomical atlas) within the liver. The resulting hepatic network (Figure 3) was obtained after 10 hours of computation.

Model parameter	Hepatic artery	Portal Vein	Hepatic vein
Blood pressure at the entry P_{in} (mmHg)	95	25	12
Blood pressure at the output P_{out} (mmHg)	20	15	5
Wall thickness ratio (fraction of vessel radius)	0.2	0.1	0.1
Hepatic blood flow (ml/min)	400	1100	1500
Size of the macro-cell (cm ³)	0.125		
Number of growth cycles	60		
Change of the liver size (Initial->Adult) (cm ³)	75 -> 1500		
Number of macro-cells in the adult liver	~12000		

Table 1. Main parameters of the model used in the simulation of the hepatic vascular network growth.

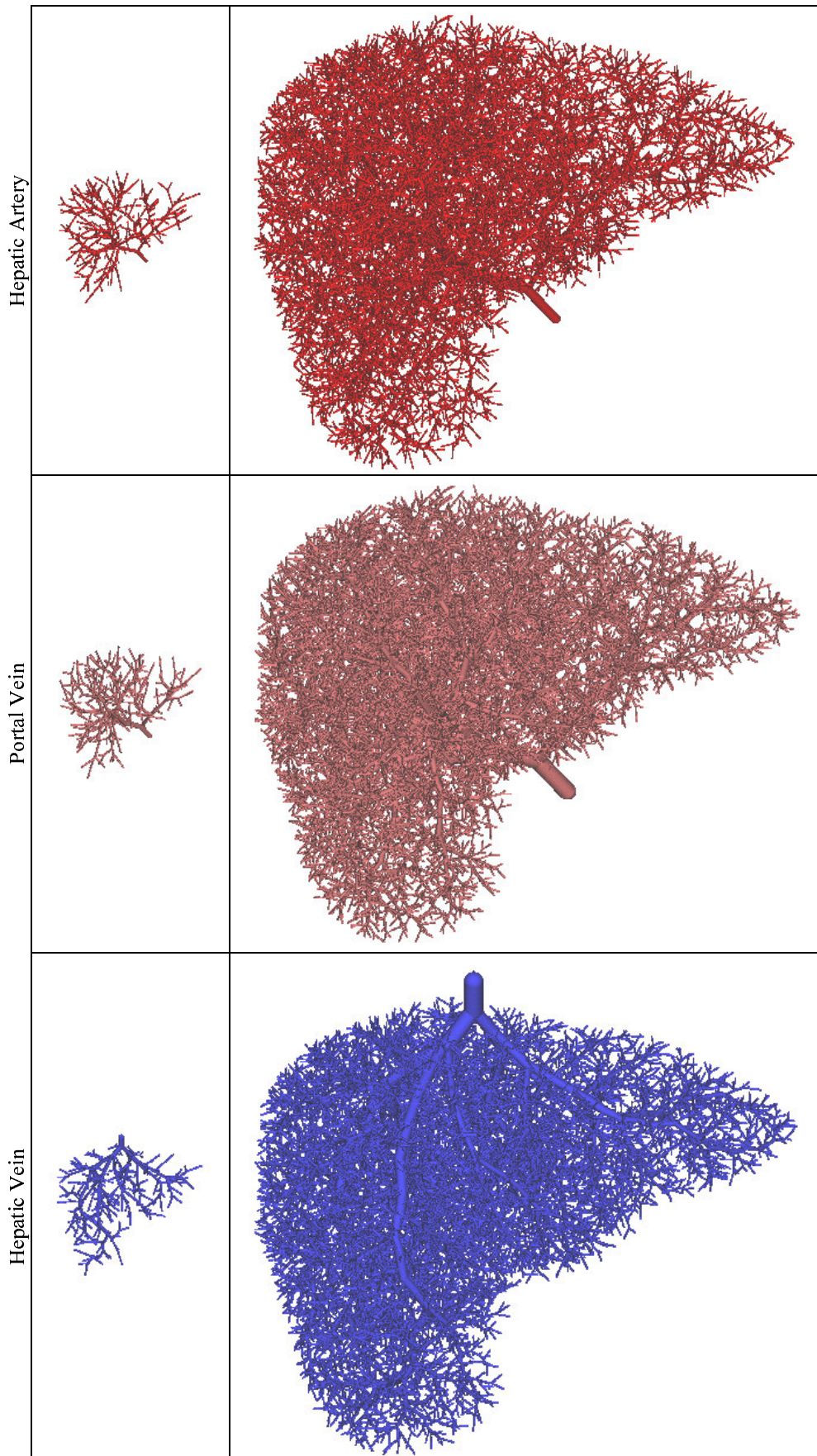


Figure 3. Results of the simulation of the hepatic vascular trees growth: in the left column trees after the first few cycles and in the right column adult trees.

3.2. Simulation of pathological processes and image acquisitions

Two situations, which are the most relevant in hepatic tumors, are studied: hyper- and hypo-vascularization. In case of a so-called hyper-vascularized tumor (e.g. *Hepatocellular Carcinoma*), the normal blood supply is strongly modified: the lesion is perfused only by HA without any PV supply and the blood flow in arteries is significantly increased. Consequently, the hyper-vascularization can be observed in HA and HV but not in the PV tree. Hypo-vascular lesions are less complicated to generate, because the death of macro-cells results in regions almost not perfused by any tree.

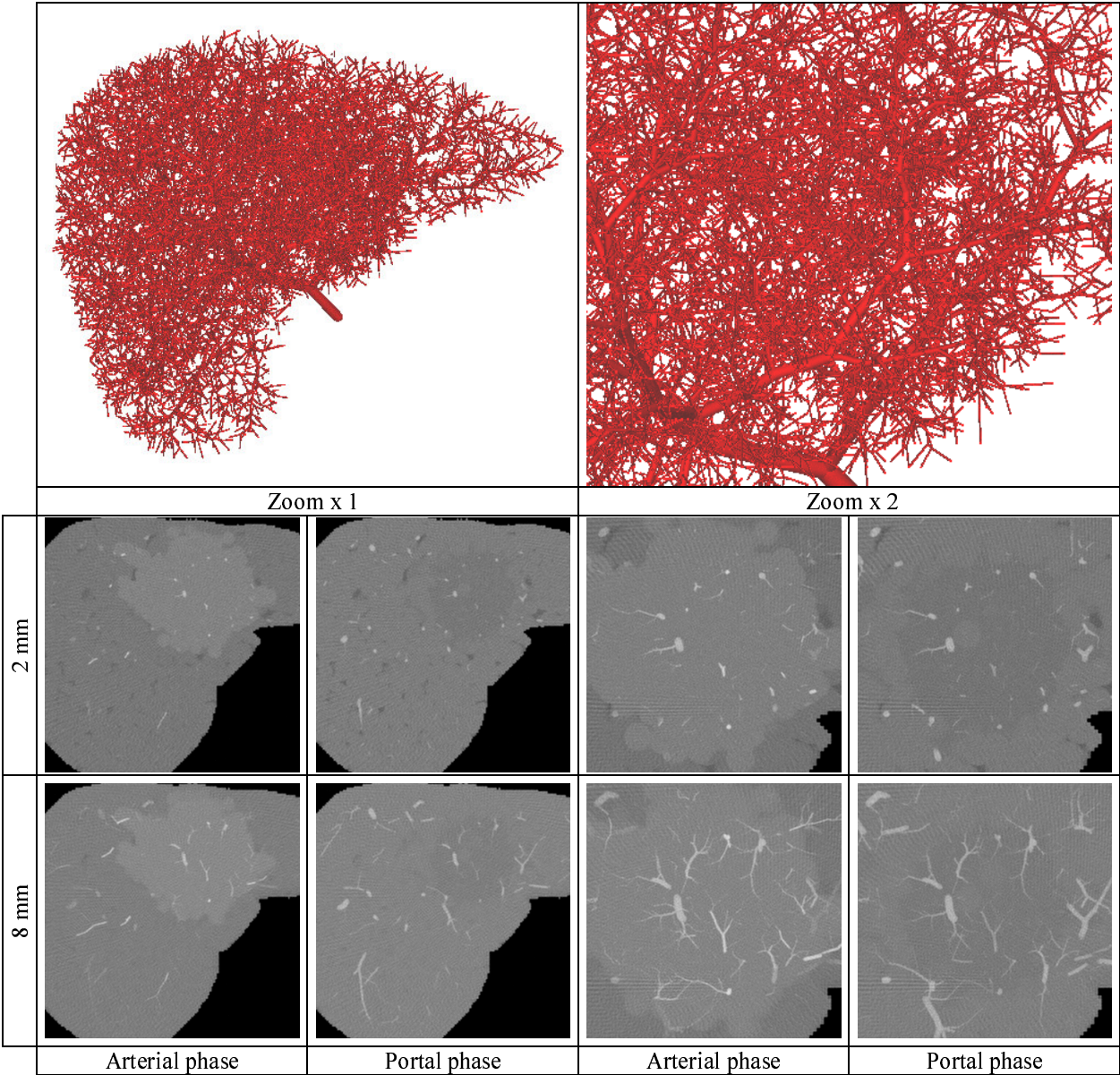


Figure 4. Arterial tree with the hyper-vascularized region and the corresponding CT scans (at arterial and portal phase with varied spatial resolution).

In both cases the pathological changes are introduced by a single conversion (lasting 5-10 cycles) during the adult phase, and then the simulation is continued for at least 10 cycles. Initialization of the simulated lesions (position and size – radius=20 mm) is the same in different experiments for comparison facilities.

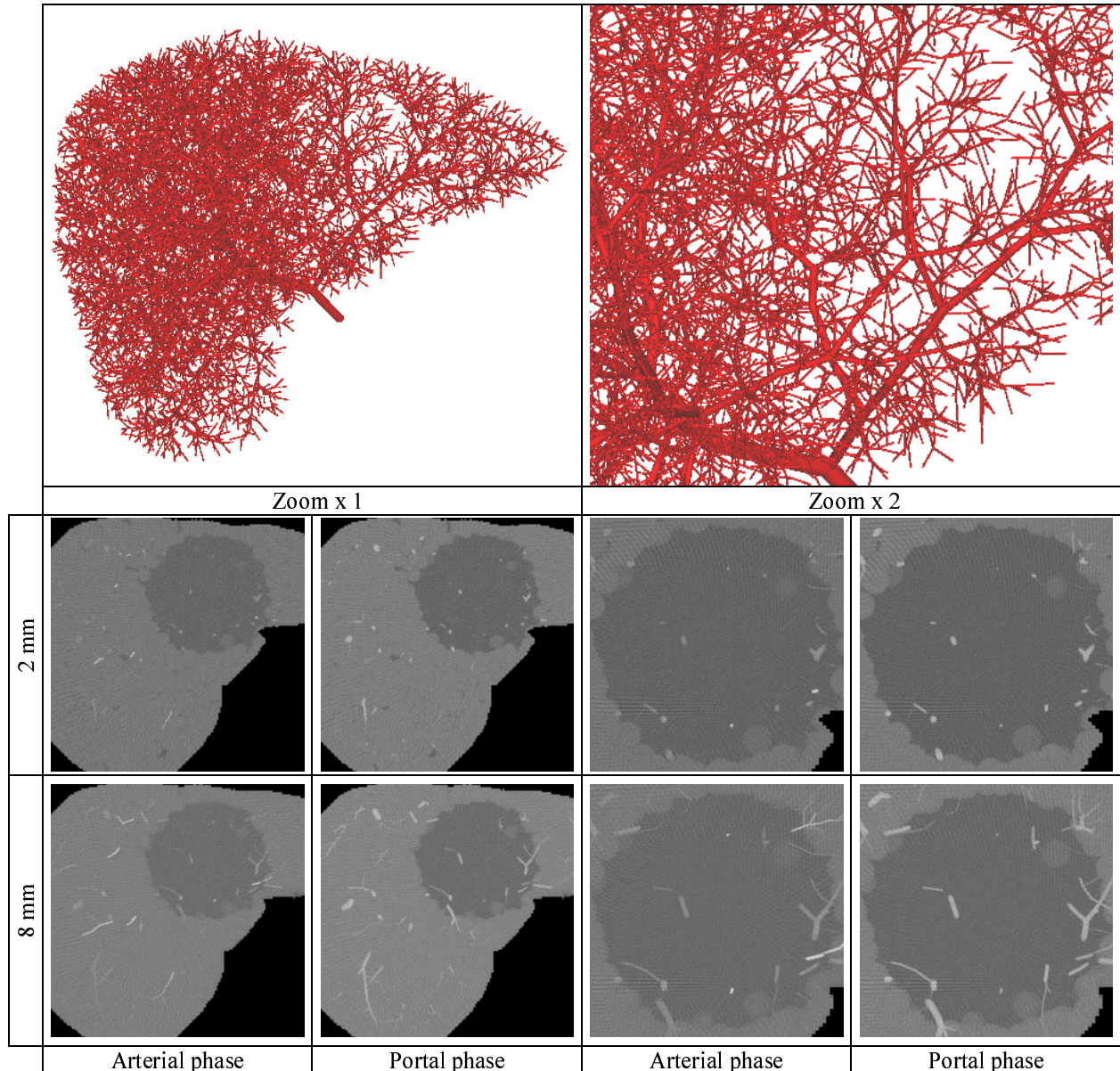


Figure 5. Arterial tree with the hypo-vascularized lesion and the corresponding CT scans (at arterial and portal phase with varied spatial resolution).

Figure 4 shows the simulation results of the hepatic arterial tree perfusing the liver with a hyper-vascular lesion. The 3D vascular tree is presented with two different resolutions (Zoom $\times 1$, Zoom $\times 2$). In the same figure, eight simulated CT scans are shown, four at each resolution. For each resolution, two images correspond to a 2 mm slice thickness, and two have been synthesized with a 8 mm thickness. Among the two images with a given thickness, one is simulated during the clinical “arterial phase” of acquisition, and the second one during

the “portal phase”. Indeed, when radiologists perform a CT examination of the liver, they acquire two series of images during the propagation of CM: the first one when only the arterial network is enhanced, called the arterial phase, and the second one, 30-40 s later when the CM arrives also in the PV, called the portal phase. As the tumor conspicuity depends strongly on the acquisition time, this double scanning allows to correctly recognize the tumor type, by precisely understanding its vascular modifications.

The simulated CT scans presented in Fig. 4 show results that are in agreement with real acquisitions: the hyper-vascular tumor appears more intense than normal parenchyma at the arterial phase and slightly hypo-dense during the portal phase, with a decreasing conspicuity.

Fig. 5 shows exactly the same kind of results for the simulated hypo-vascular lesion. This time, the tumor is hypo-dense at the two phases, which also corresponds to real data.

3.3. Texture analysis of simulated CT scans

A visual inspection of the simulated images shows already significant differences among scans acquired with different parameters (spatial resolution, slice thickness and time). On the 2 mm thick slices, vessels resemble dots, whereas on thicker ones, segments and bifurcations can be easily discerned. In addition, when the spatial resolution is increased (by zooming) the number of visible details is augmented. It can be expected that some textural features will vary with changes of acquisition conditions. In order to study their evolution with these parameters, the calculation of features is conducted for 8 slice thicknesses (1 to 8 mm), 6 resolutions ($\times 1.0$ to $\times 2.0$) and 2 time instants (corresponding roughly to the arterial and portal phase), which gives almost 100 combinations.

Circular, large (50 pixels radius) ROI-s are placed in the center of lesions and in the normal tissue. Textural features obtained by classical statistical methods (first order, gradient based, co-occurrence and run-length matrix based) [22], [23] were computed. The features corresponding to four angles (0° , 45° , 90° and 135°) (e.g. all derived from run-length matrix) were averaged.

In figures 6 and 7, the evolution of two features, according to the slice thickness and the zoom, is shown at 2 acquisition times. The first one is the well-known “average of gray levels”. Even if it gives information only on the image density, and not exactly on the spatial repartition of the gray levels, it is important to mention it in this particular case; it is often used by radiologists to detect and characterize the tumor. The second one, the “gray level

distribution”, is derived from the run-length matrix. On each graph, feature values corresponding to normal tissue are compared with those of the pathological lesion.

In case of a hyper-vascular tumor, the average gray level of the lesion is higher in the full range of the tested resolutions during the arterial phase, and a completely reversed situation can be observed during the portal phase. Considering the gray level distribution, it can be noticed that the two surfaces, describing the evolution of this feature, intersect in a similar way in both phases. Regarding a hypo-vascular tumor, the textural features seem to be less dependent on the acquisition time: a very similar evolution is observed in both phases.

These results confirm that different acquisition conditions of CT scanning influence strongly the texture observed on images. They also point out that textural features can potentially be used for discrimination purposes in clinical examinations, but only when the same (or at least similar) protocols are used.

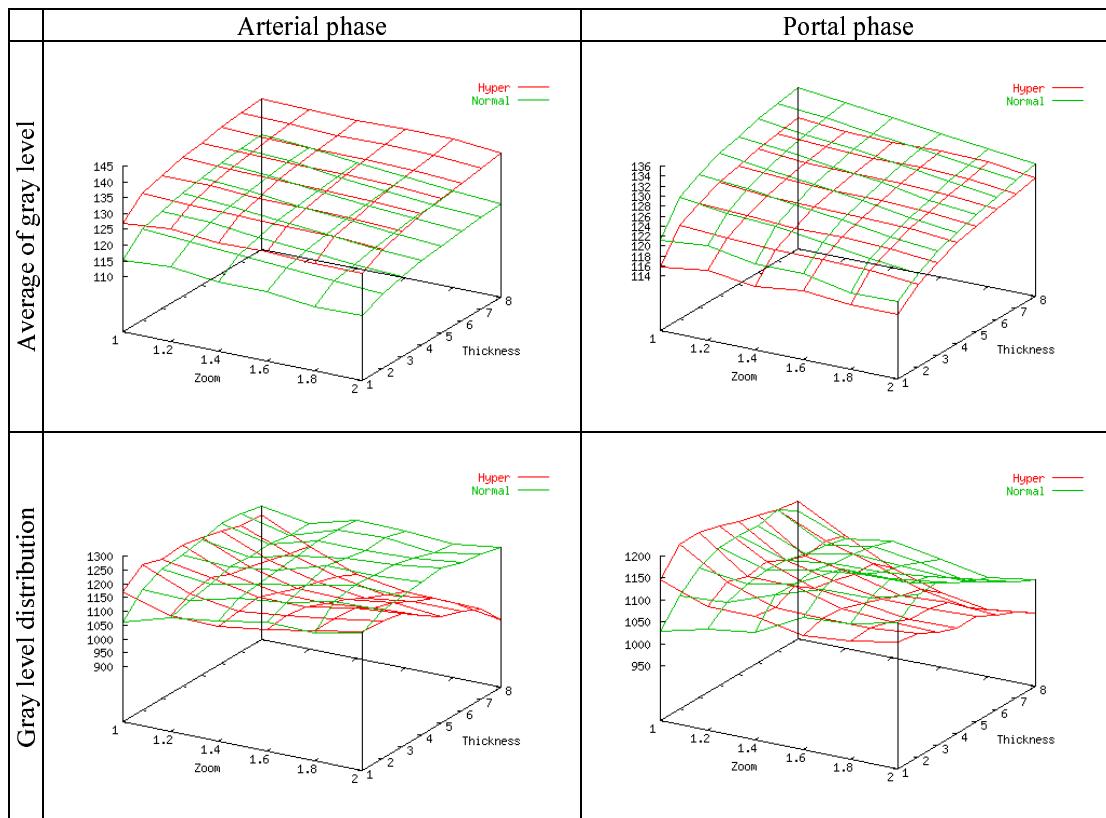


Figure 6. Evolution of two textural features (average of gray level and gray level distribution) with slice thickness and resolution, at arterial (left column) and portal (right column) times. On each graph, feature values calculated inside the hyper-vascular lesion are confronted with those corresponding to normal tissue.

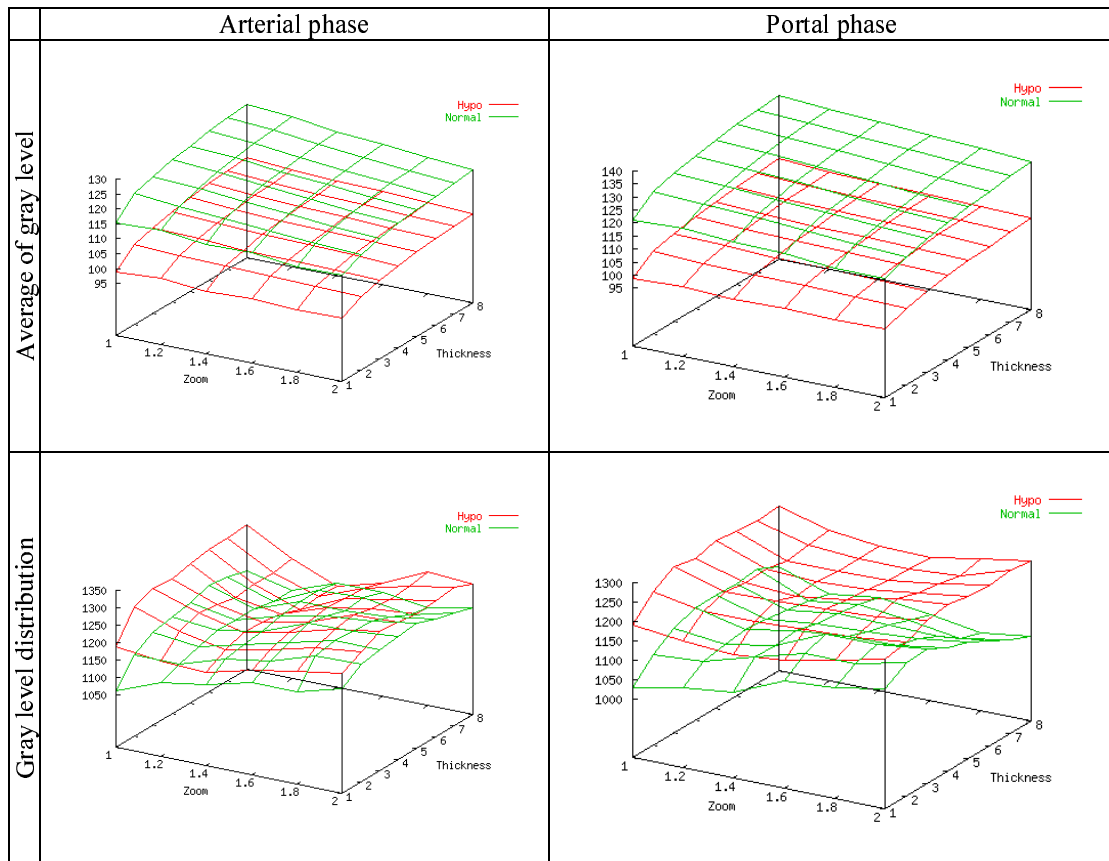


Figure 7. The same results as in figure 6, for hypo-vascular lesion.

4. Conclusions and future research

In this paper, a model-based approach of medical images interpretation has been described in order to better understand both advantages and limitations of texture analysis. It consists of two coupled models (hepatic network and CT-scan modality) which enable to perform studies corresponding to normal and pathological situations, observed by means of CT slices. In clinical conditions, the evaluation of such physiological and acquisition variations is almost impossible.

At each stage of the above method, improvements can be brought in. Considering the model of the liver, the pathological changes were simulated in a very simple way. The time-dependent evolution of lesions can be more precisely defined, which will allow to investigate e.g. a semi-automatic method for an early detection of tumors on dynamic CT images. Regarding the contrast material propagation at the macro-cell level, parenchyma enhancement can be refined by introducing compartment models.

An application of the classification methods (e.g. multivariate decision trees) based on textural features extracted from the simulated and real hepatic CT images can complete this model based methodology. A database of dynamic liver scans is continuously enlarged with the collaboration of CHU Rennes and could be used in the validation of the proposed approach.

Acknowledgements: The authors are grateful to Prof. Jean-Louis Coatrieux and Prof. Leon Bobrowski for their support and useful comments. They also thank Dr. Yan Rolland for his clinical contribution to this study. This work has been supported by Polonium Program, between France and Poland.

References:

- [1] A. Bruno, R. Collorec, J. Bézy-Wendling, P. Reuzé and Y. Rolland, "Texture analysis in medical imaging", in "Contemporary Perspectives in Three-dimensional Biomedical Imaging", C. Roux and J.L. Coatrieux (Eds.), IOS Press, pp. 133-164, 1997.
- [2] S. Herlidou, Y. Rolland, J.Y. Bansard, E. Le Ruleur and J.D. de Certaines "Comparison of automated and visual texture analysis in MRI: Characterization of normal and diseased skeletal muscle", *Magnetic Resonance Imaging*, 17(9), pp. 1393-1397, 1999.
- [3] F. Lefebvre, M. Meunier, F. Thibault, P. Laugier and G. Berger, "Computerized ultrasound B-scan characterization of breast nodules", *Ultrasound in Medicine and Biology*, 26(9), pp. 1421-1428, 2000.
- [4] D. Chappard, A. Chennebault, M. Moreau, E. Legrand, M. Audran and M.F. Basle, "Texture analysis of X-ray radiograms is a more reliable descriptor of bone loss than mineral content in a rat model of localized disuse induced by the Clostridium botulinum toxin", *Bone*, 28(1), pp. 72-79, 2001.
- [5] M.F. McNitt-Gray, N. Wyckoff, J.W. Sayre, J.G. Goldin and D.R. Aberle, "The effects of co-occurrence matrix based texture parameters on the classification of solitary pulmonary nodules imaged on computed tomography", *Computerized Medical Imaging and Graphics*, 23, pp. 339-348, 1999.
- [6] D.G. Vince, K.J. Dixon, R.M. Cothren and J.F. Cornhill, "Comparison of texture analysis methods for the characterization of coronary plaques in intravascular ultrasound images", *Computerized Medical Imaging and Graphics*, 24, pp. 221-229, 2000.
- [7] C.D. Murray, "The physiological principle of minimum work applied to the angle of branching arteries", *J. Gen. Physiol*, 9, pp. 835-841, 1926.
- [8] M.E. Gottlieb, "Modeling blood vessels: a deterministic method with fractal structure based on physiological rules", *Proc. Int. Conf. of the IEEE Engineering in Medicine and Biology Society*, 12 (3), pp.1386-7, 1990.
- [9] W. Schreiner and P.F. Buxbaum, "Computer optimization of vascular trees", *IEEE Transactions on Biomedical Engineering*, 40(5), pp. 482-91, 1993.

- [10] F. Nekka, S. Kyriacos, C. Kerrigan and L. Cartilier, “A model of growing vascular structures”, *Bull. Math. Biol.*, 58(3), pp. 409-24, 1996.
- [11] R. Karch, F. Neumann, M. Neumann and W. Schreiner, “A three-dimensional model for arterial tree representation, generated by constrained constructive optimization”, *Computers in Biology and Medicine*, 29, pp. 19-38, 1999.
- [12] J. Bézy-Wendling and A. Bruno, “A 3-D dynamic model of vascular trees”, *Journal of Biological Systems*, 7(1), pp. 11-31, 1999.
- [13] Y. Rolland, J. Bézy-Wendling, R. Duvauferrier and J.L. Coatrieux, “Slice simulation from a model of the parenchymous vascularization to evaluate texture features”, *Investigative Radiology*, 34(3), pp. 181-184, 1999.
- [14] J. Bézy-Wendling, M. Krętowski, Y. Rolland and W. Le Bidon, “Toward a better understanding of texture in vascular CT scan simulated image”, *IEEE Transactions on Biomedical Engineering*, 48(1), pp. 120-124, 2001.
- [15] O. Hudlicka, M.D. Brown and S. Egginton, “Angiogenesis: basic concepts and methodology”, in *An Introduction to Vascular Biology*, edited by A. Halliday, B.J. Hunt, L. Poston and M. Schachter, Cambridge University Press, pp. 3-19, 1998.
- [16] M. Zamir, “Optimality principles in arterial branching”, *J. Theor. Biol.*, 62, pp. 227-251, 1976.
- [17] M.A. Changizi and C. Cherniak, “Modeling the large-scale geometry of human coronary arteries”, *Can. J. Physiol. Pharmacol.*, 78, pp. 603-611, 2000.
- [18] A. Kamiya and T. Togawa, “Optimal branching structure of the vascular trees”, *Bulletin of Mathematical Biophysics*, 34, pp. 431-438, 1972.
- [19] M. Krętowski, Y. Rolland, J. Bézy-Wendling and J.L. Coatrieux, “Fast algorithm for 3-D vascular tree modeling”, *Computer Methods and Programs in Biomedicine* (in print), 2002.
- [20] G.T. Herman, “Image Reconstruction from Projections, The Fundamentals of Computerized Tomography”, *Computer Science and Applied Mathematics*, 1980.
- [21] A.C. Kak, M. Slaney, “Principles of Computerized Tomographic Imaging”, IEEE Press, 1988.
- [22] R.M. Haralick, K. Shanmugam and I. Dinstein, “Textural features for image classification”, *IEEE Transactions on Systems, Man and Cybernetics*, 3, pp. 610-621, 1973.
- [23] R.M. Haralick, “Statistical and structural approaches to texture”, *Proceedings of the IEEE*, 67(5), pp. 786-804, 1979.